ADVANCED MATERIALS

Supporting Information

for *Adv. Mater.*, DOI: 10.1002/adma.201805088

Tailor-Made Microporous Metal–Organic Frameworks for the Full Separation of Propane from Propylene Through Selective Size Exclusion

*Hao Wang, Xinglong Dong, Valentina Colombo, Qining Wang, Yanyao Liu, Wei Liu, Xin-Long Wang, Xiao-Ying Huang, Davide M. Proserpio, Angelo Sironi, Yu Han, and Jing Li**

Supporting Information

Tailor-Made Microporous Metal-Organic Frameworks for the Full Separation of Propane from Propylene Through Selective Size Exclusion

*Hao Wang, Xinglong Dong, Valentina Colombo, Qining Wang, Yanyao Liu, Wei Liu, Xin-Long Wang, Xiao-Ying Huang, Davide M. Proserpio, Angelo Sironi, Yu Han, and Jing Li**

Experimental Details

General Information: All reagents were used as received unless otherwise specified. ^{1}H NMR data were collected on a 300 MHz Oxford NMR unit. X-ray single-crystal data collection of Y-bptc was obtained on a Bruker D8 Venture diffractometer equipped with a graphite monochromator using Mo Kα radiation (λ = 0.71073 Å) at 173 K. A multiscan technique was used to perform adsorption corrections. The crystal structure was solved using direct methods and refined using the full matrix least-squares method on F^2 with anisotropic thermal parameters for all non-hydrogen atoms using the SHELXL-2014 program. All hydrogen atoms were located in calculated positions and refined isotropically. Powder X-ray diffraction patterns were recorded on a Ultima IV with Cu Kα radiation (λ= 1.5406 Å). Data were collected at room temperature at 2θ = 3-40° with a scan speed of 2°/min and operating power of 40 kV and 44 mA. For structure solution process, PXRD data were collected on a Bruker AXS D8 Advance diffractometer (of the University of Milan, see next pharagraph). Thermogravimetric analysis was carried out on a Q5000 (TA Instruments) analyzer. For each run 3-4 mg of sample was heated from room temperature to 600 °C at a ramp rate of 10 °C/min. N_2 adsorption experiments at 77 K and CO_2 adsorption measurements at 195 K were performed on a Micromeritics 3Flex adsorption analyzer with liquid nitrogen and dry ice/ isopropanol as coolants, respectively. Prior to each measurement, ~ 100 mg of solvent exchanged sample was activated at 200 or 300 ^{o}C under dynamic vacuum overnight.

Thermodiffractomery: Variable-temperature X-ray powder diffraction (VT-PXRD) experiments were performed on Y-abtc. The experiment was carried out under N_2 flux by coupling a custom-made sample heater, assembled by Officina Elettrotecnica di Tenno, Ponte Arche, Italy, to the instrumental set-up described above. Powdered microcrystalline sample of Y-abtc was ground in an agate mortar and was deposited in the hollow of on a quartz zero-background plate framed by an aluminum skeleton. The data were acquired within a sensible, low-angle 2θ range (9-30°), heating the samples in situ in the temperature range RT-540 °C, with steps of 20 °C, under nitrogen flux. The N_2 atmosphere on the sample was insured by a home-made dome that fits on the sample holder and allow the X-rays to reach the sample through Kapton windows. Le Bail parametric refinements on the data measured in the range 30-540 °C (i.e. before a significant loss of crystallinity was observed) allowed describing the behavior of the unit cell parameters as a function of the temperature. The VT diffractograms and the results of the parametric data treatments are depicted in Supplementary Note 2. It should be noted that when comparing TGA and VTXRPD results, the reader must be aware that the thermocouple of the VT-PXPD set-up is not in direct contact with the sample, this determining a slight difference in the temperature at which the same event is detected by the two techniques. The TGA temperatures have to be considered as more reliable.

Hydrocarbon adsorption measurements: Hydrocarbon adsorption isotherms were collected with a volumetric gas sorption analyzer, Autosorb-1 (Quantachrome Instruments). Analysis temperature (25-80 °C) was controlled by a circulating-bath temperature controller. For a typical isotherm, around 150 mg of the solvent-exchanged sample was used and activated prior to data collection. Hydrocarbon adsorption rate measurements were performed on a gravimetric adsorption unit modified from a Q50 thermogravimetric analyzer (TA Instruments). For each measurement, ~ 20 mg of MOF sample was activated under nitrogen flow for 2 hours to remove any residual solvent. After cooling down to the adsorption temperature, hydrocarbon flow was mixed with the pure nitrogen stream and then introduced to the adsorption chamber mained at analysis temperature. Hydrocarbon partial pressure was controlled by adjusting the relative flow rates of the two gas streams (pure nitrogen and pure hydrocarbon). Sample weight was recorded throughout the process which gives the information of the adsorbed amount of the adsorbate.
Column breakthrough experiments: Multicomponent column breakthrough experiments were conducted using a lab-scale fix-bed packed with the MOF sample. For a typical experiment, 0.53 g of MOF material was packed into a quartz column (5.8 mm I.D. ×150 mm) with silane treated glass wool filling the void space. A helium flow was used to for initial purging of the adsorbent. The MOF powder was activated at 200 °C overnight and the helium flow was then turned off while propane and propylene flows were introduced. Flow rates of each gas were adjusted to control the composition of the feed gas mixture. The effluent from the column was monitored using an online GC equipped with HP-PONA column and FID. The absolute adsorbed amount of gas i (*qi*) is calculated from the breakthrough curve by the equation:

$$q_i = \frac{F_i \times t_0 - V_{dead} - \int_0^{t_0} F_e \Delta t}{m}$$

Where Fi is the influent flow rate of the specific gas (cm^3/min); t_0 is the adsorption time (min); V_{dead} is the dead volume of the system (cm^3); F_e is the effluent flow rate of the specific gas (cm^3/min); and m is the mass of the sorbent (g).

Ab initio structure solution from powder XRD data: Gently ground powders of Y-abtc compound were deposited in the, 2 mm deep, hollow of a zero background plate (a properly misoriented quartz monocrystal). Diffraction experiments were performed at the University of Milan (Italy), using Cu-Kα radiation (λ = 1.5418 Å) on a vertical-scan Bruker AXS D8 Advance diffractometer in θ:θ mode, equipped with a Goebel Mirror and a linear Position Sensitive Detector (PSD), with the following optics: primary and secondary Soller slits, 2.3° and 2.5°, respectively; divergence slit, 0.1°; receiving slit, 2.82°. Generator setting: 40 kV, 40 mA. The nominal resolution for the present set-up is 0.08° 2θ (FWHM of the α1 component) for the LaB_6 peak at about 21.3° (2θ). The accurate diffraction patterns at RT and under nitrogen flow were acquired in the 5–105° 2θ range, with Δ2θ = 0.02° and exposure time 10 s/step with the same chamber used for the thermodiffraction experiment.

Structural analysis process. A standard peak search below 30° was followed by indexing through the singular value decomposition method, implemented in TOPAS, which led to a rhombohedral cell of approximate dimensions: a = 18.09 Å , b = 45.36 Å, c = 10.84Å and V = 12860 $Å^3$ (GOF(20) = 28.77). A Le Bail refinement of the pattern in *R*-3 gives rise to a slightly better R_{wp} than in *R*-3*c*. However, all peaks were already correctly described by the *R*-3*c* space group,. The slightly better fitting for *R*-3 is indeed simply due to the presence of unobserved peaks that contributes only to the modelling of the background. The determination of the background, correct unit cell parameters, sample displacement and profile parameters to be used in the subsequent simulated annealing runs, was indeed done on the basis of these structureless Le Bail refinements. The correctness of the *R*-3*c* space group was eventually confirmed by the successful two-step simulated annealing approach. Indeed, in the first run, we

localized the [$Y_6(\mu_3\text{-}OH)_8$] moiety, centred around a Wyckoff position *b*, and described by one Y and one O atom in general position and another O atom on a three-fold axis (Wyckoff site *c*). In the second step, we located the position of the abtc ligand, by using a flexible rigid body (Figure S7) consisting of the full ligand with halved occupancy, with its center of mass on a *d* Wyckoff site. Once confirmed to be the right position of the ligand, this was better described by half ligand with full occupancy. However, the obtained structural model, even if coherent for atom connectivity and for congruency with the Y-bptc cubic MOF, ended with a high R_{wp} = 30. We ascribed this to the high porosity of the Y-abtc MOF, in which the voids are, in the as synthesized form, filled by solvent molecules and dimethyl ammonium cations, that contributes to the overall intensity of the diffraction peaks. Indeed, to try to work on better data coming from a partially activated sample, a first quick thermodiffraction experiment was performed, with heating steps of 50 °C from RT to 320 °C, under N_2 flux. The temperature was than kept at 320 °C for 5 hours and the powder was cooled to room temperature for a new overnight scan (by keeping the N_2 flux on the sample). The same structural model, refined on the new data set, reached a promising R_{wp} of 13.12. A subsequent Rietveld refinement with freely floating water oxygen atom, with a refinable site occupancy factor, revealed the presence of the oxygen of the coordinated water molecule (with occupancy 0.52) at the Y site. Moreover, the contemporary presence of residual electron density into the voids was described by freely roto-translating dummy C atoms, with refinable occupancy, with the aim of simulating the presence of the extra framework cations. This let to refine the powder diffraction pattern to a satisfactory R_{wp} = 11.41. During these Rietveld refinement steps, torsional angles around the C1-N1; C5-C8 and C3-C7 bonds were let to refinePeak shapes were described with the fundamental parameters approach and with the aid of 4th-order spherical harmonics. Moreover, the background was modelled by a Chebyshev polynomial function. The thermal effect was simulated by using a single isotropic parameter for the metal ion, augmented by 2.0 Å^2 for lighter atoms. The final Rietveld refinement plot are supplied in Figure S5. Crystal data are reported in the text. Fractional atomic coordinates are provided with the Supporting Information as CIF file.

Synthesis of H_4bptc

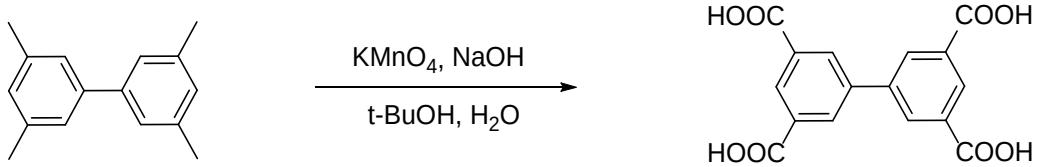

3,3'5,5'-tetramethylbiphenyl (5.0 g, 0.023 mol), NaOH (2.0 g, 0.05 mol) were mixed in t-BuOH/H_2O (100/100 mL) with stirring at 50 °C. $KMnO_4$ (43.0 g, 0.27 mol) was added in portions over one week. The temperature was subsequently increased to 70 °C and kept for 2 days. The mixture was filter when hot and the clear filtrate was added into 100 mL 6M HCl. White solid was obtained upon filtration. The crude product was recrystallized from DMF (~100 mL) to give pure H_4bptc with a yield 82%. ^{1}H NMR (400 MHz, DMSO-d^6): δ= 13.50 (4H, COOH), 8.51 (2H, Ar-H), 8.42 (4H, Ar-H).

Synthesis of H_4abtc

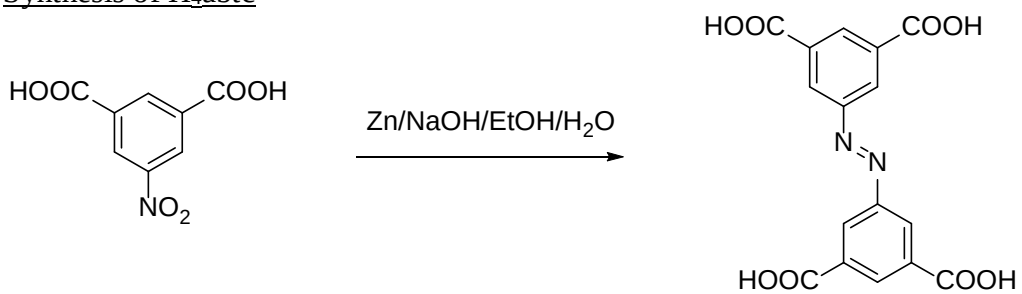

5-nitroisophthalic acid (2.1 g, 0.01 mol), NaOH (3.2 g, 0.08 mol), Zinc powder (2.1 g, 0.04 mol) were mixed in ethanol/H_2O (50/20 mL). The mixture was kept under refluxing for 12 hours before cooled to room temperature. Yellow solid was obtained through vacuum filtration which was then dissolved in 80 mL 1M NaOH solution. Upon filtration, the filtrate was acidified with 6 M HCl to get orange solid. The crude product was recrystallized from DMF to give pure H_4abtc as orange solid (1.3 g, yield: 73%). ^{1}H NMR (400 MHz, DMSO-d^6): δ= 13.38 (4H, COOH), 8.58-8.61 (6H, Ar-H).

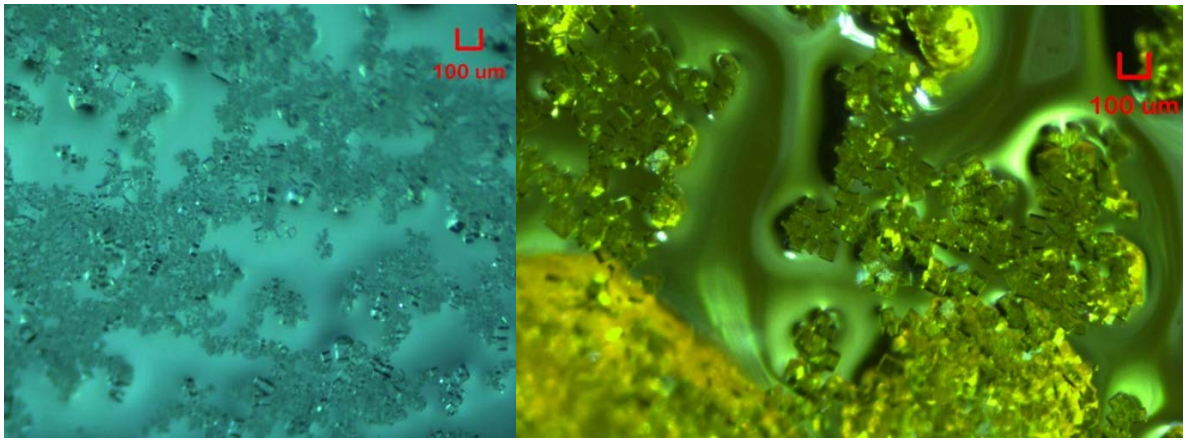

Figure S1. Microscopic images of crystals of Y-bptc (left) and Y-abtc (right).

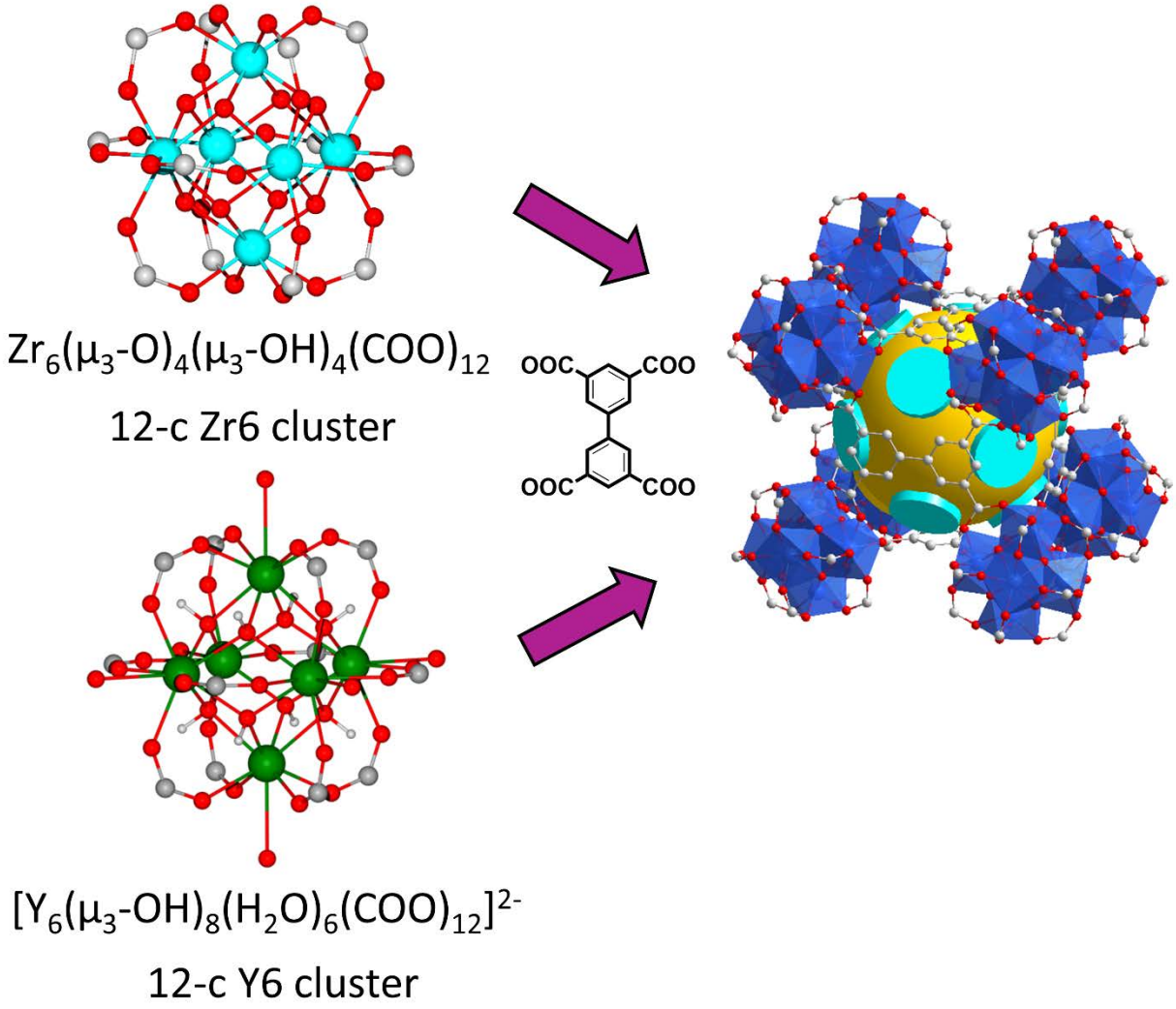

Figure S2. Comparison of Zr-bptc and Y-bptc. They are both built on 12-connected hexanuclear SBU and share similar connectivity and topology. But the two inorganic clusters are different in terms of composition and coordination.

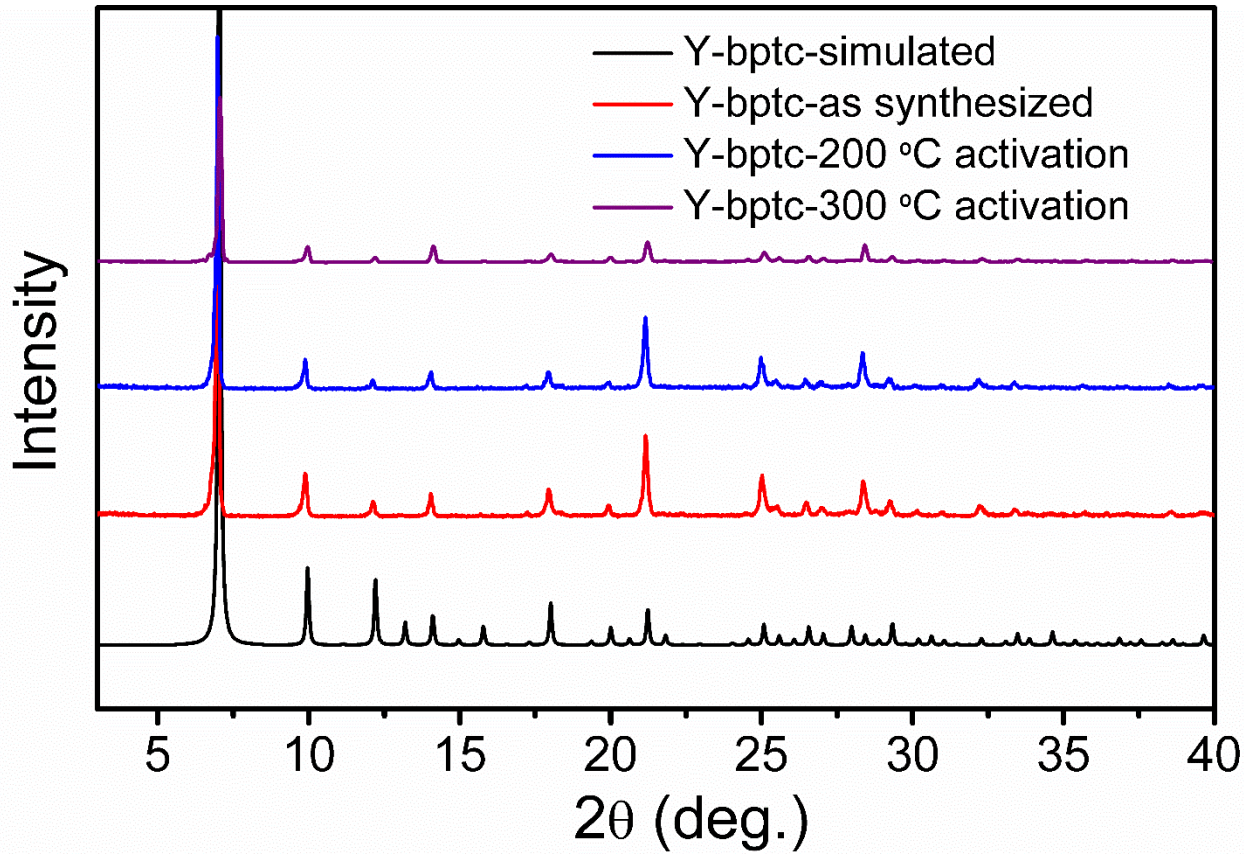

Figure S3 PXRD patterns for Y-bptc.

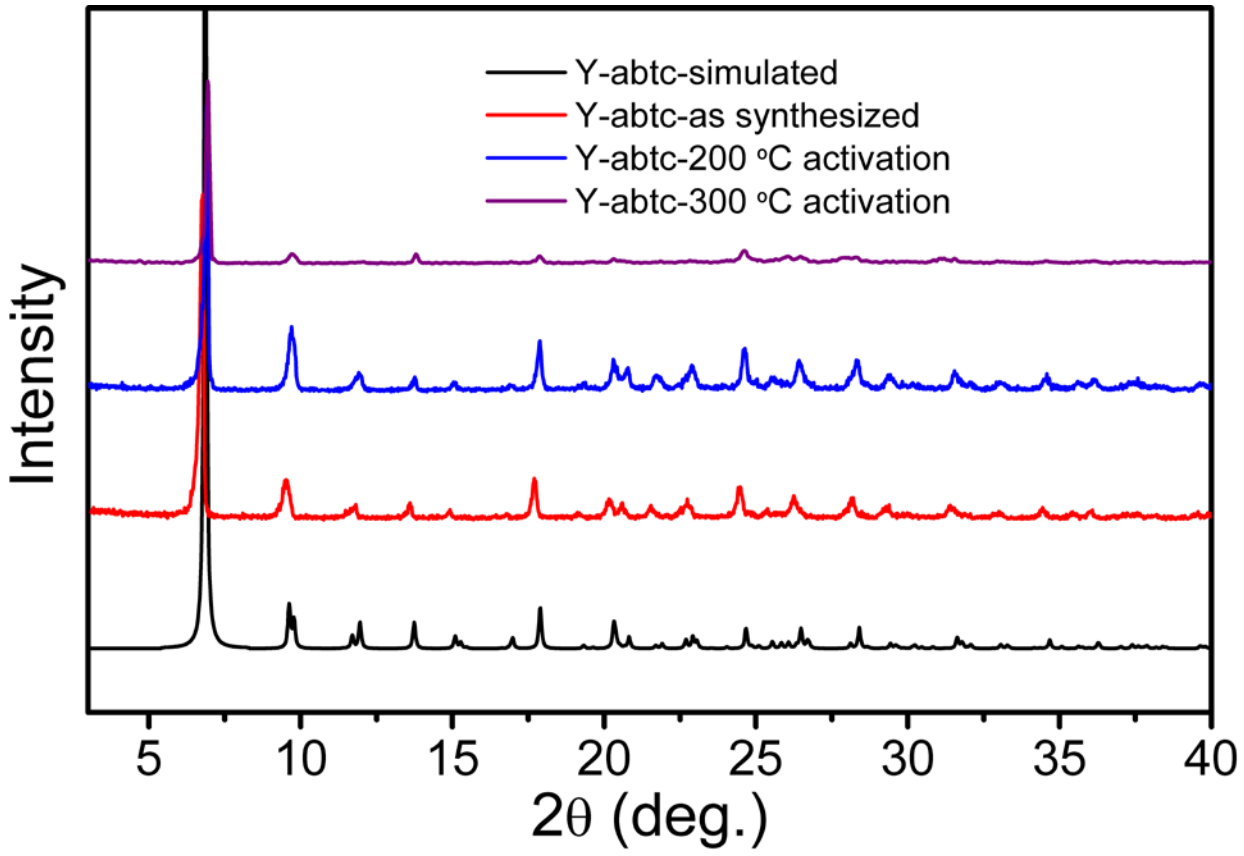

Figure S4. PXRD patterns for Y-abtc.

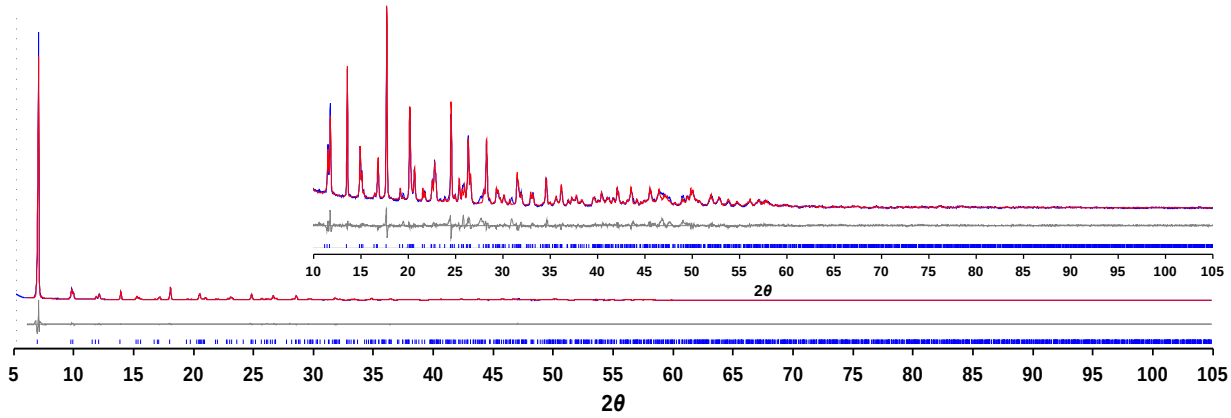

Figure S5. Final Rietveld Refinement plot for Y-abtc. Blue line, experimental data; red line, calculated; gray line, difference between experimental and calculated patterns. Blue tick marks represent peaks positions. The inset show a magnification of the high angle region. R_p and R_{wp} = 0.0754 and, 0.1022 for 5001 data collected in the 5–105° 2θ range. R_{Bragg} = 2.22.

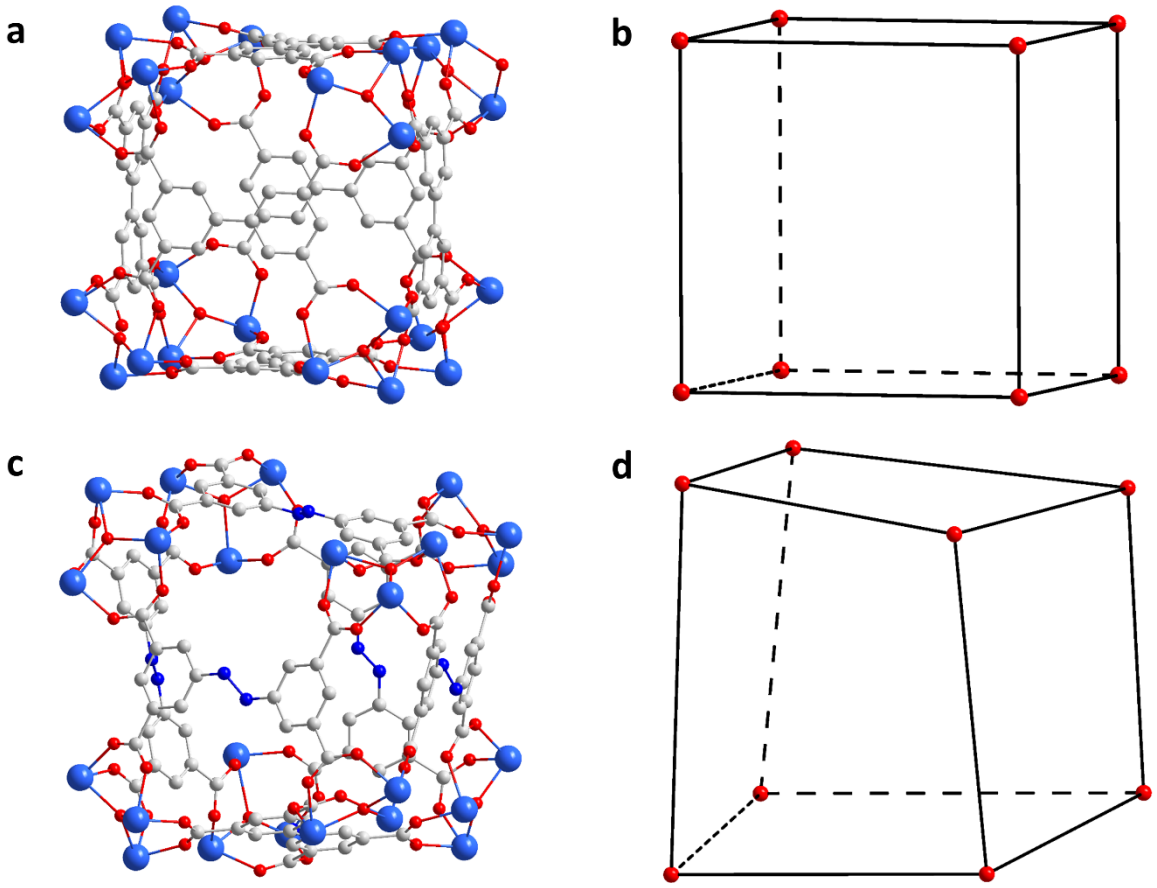

Figure S6. Crystal structure of a single cage and the shape of the cage depicted by connecting eight equivalent μ_3-O atom from the vertexes of the cage for Y-abtc (a, b) and Y-bptc (c, d).

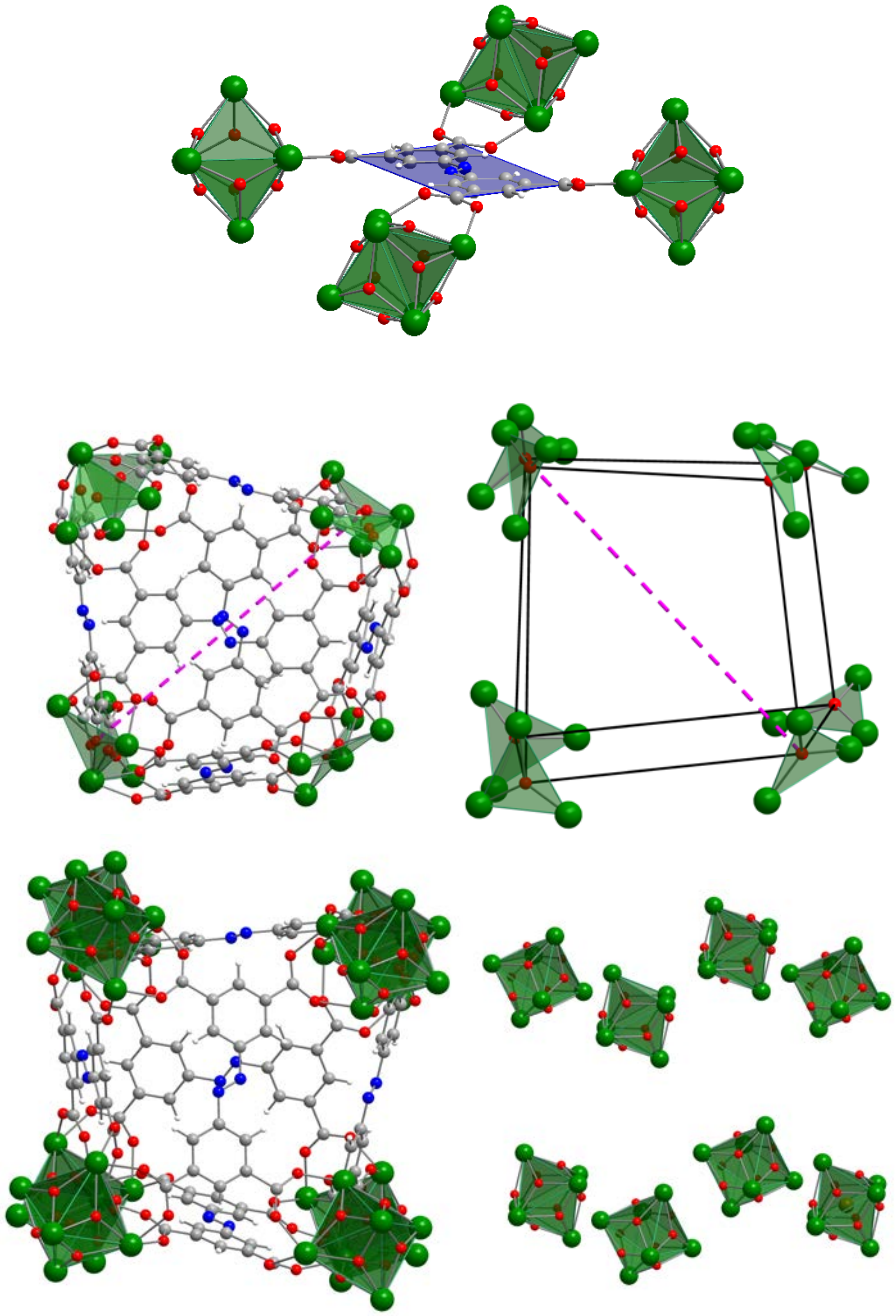

Figure S7. Coordination geometry of abtc and the distortion of the cages in Y-abtc. In this picture, the 3 fold axis is represented by the fragmented pink line.

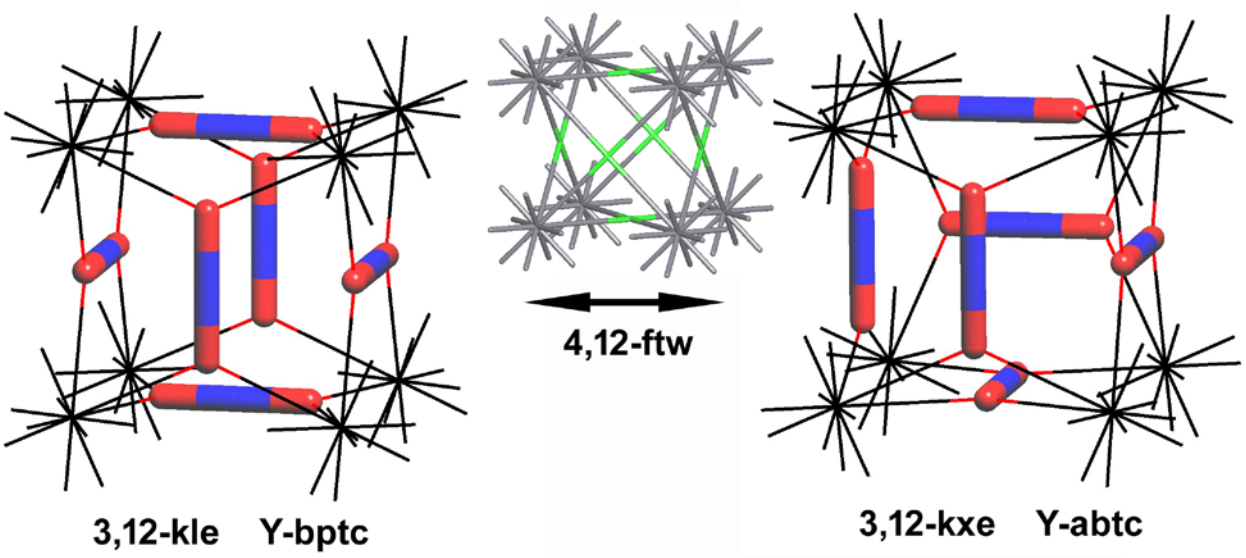

Figure S8. Comparison of 3,12-**kle** and 3,12-**kxe** nets derived from 4,12-**ftw**.

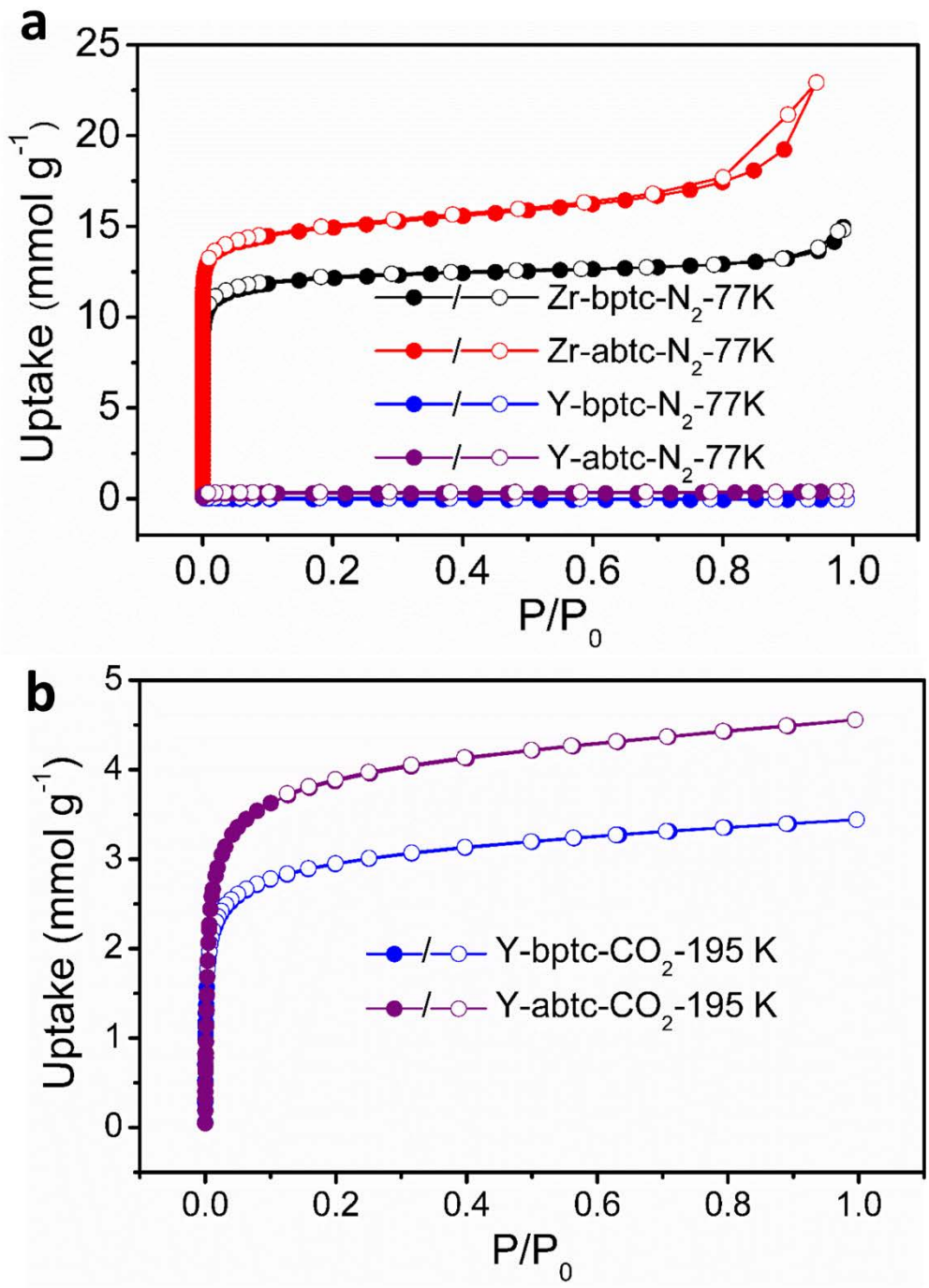

Figure S9. a) N_2 adsorption-desorption isotherms of Zr-bptc and Zr-abtc at 77 K. b) CO_2 adsorption-desorption isotherm of Y-bptc and Y-abtc at 195 K.

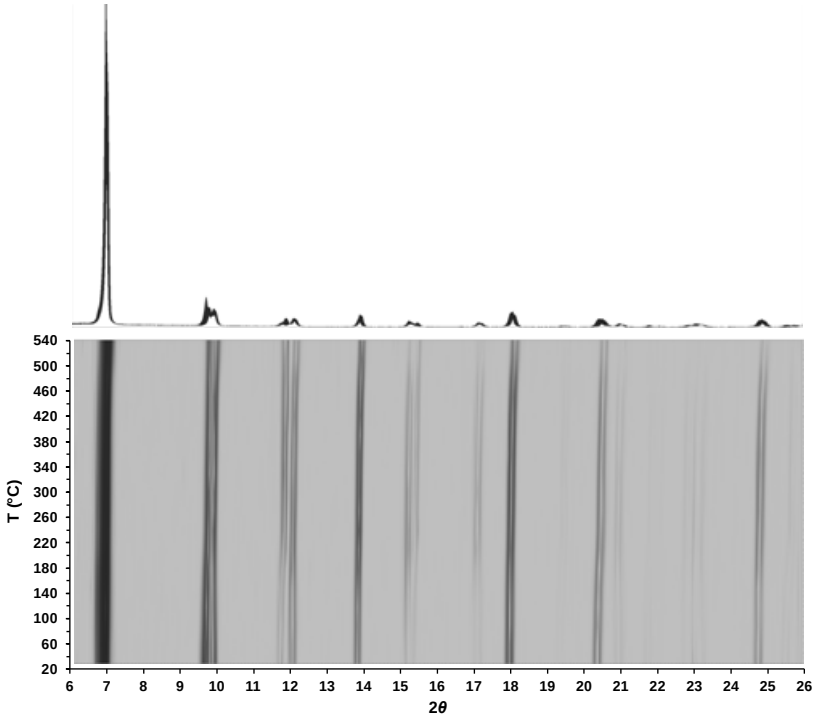

Figure S10. Head-on overlaid powder X-ray diffraction patterns measured at elevating temperatures in the range 20-540 °C for Y-abtc (top) and its two-dimensional contour plot as a function of 2θ and temperature (bottom), displaying the thermal stability. Notably, the diffraction patterns remained unaltered during the measurements except for minor changes in peak intensity.

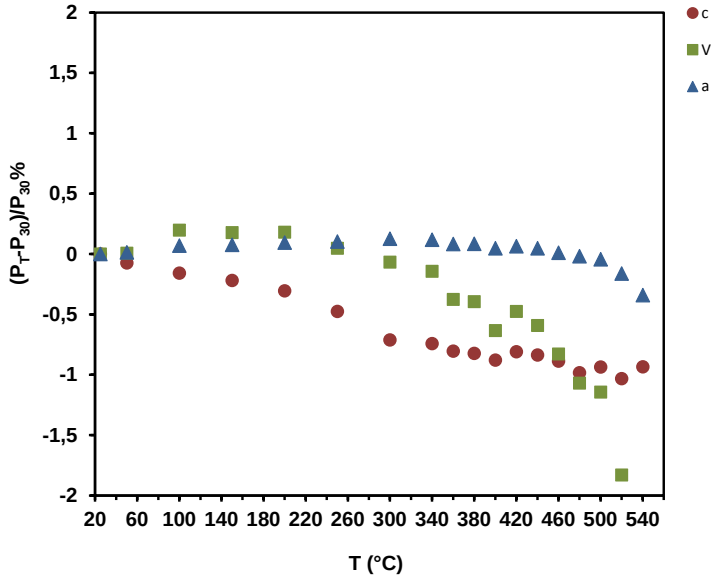

Figure S11. Variation of the unit cell parameters (P_T), normalized to the value at 30 °C (P_{30}), as a function of the temperature in the range 30-540 °C. **a**, blue triangles; **c**, red circles; **V**, green squares. This graph shows that the framework is substantially rigid, only a small (-2%) volume contraction is observed up to 520 °C (temperature at which the framework start losing its crystallinity).

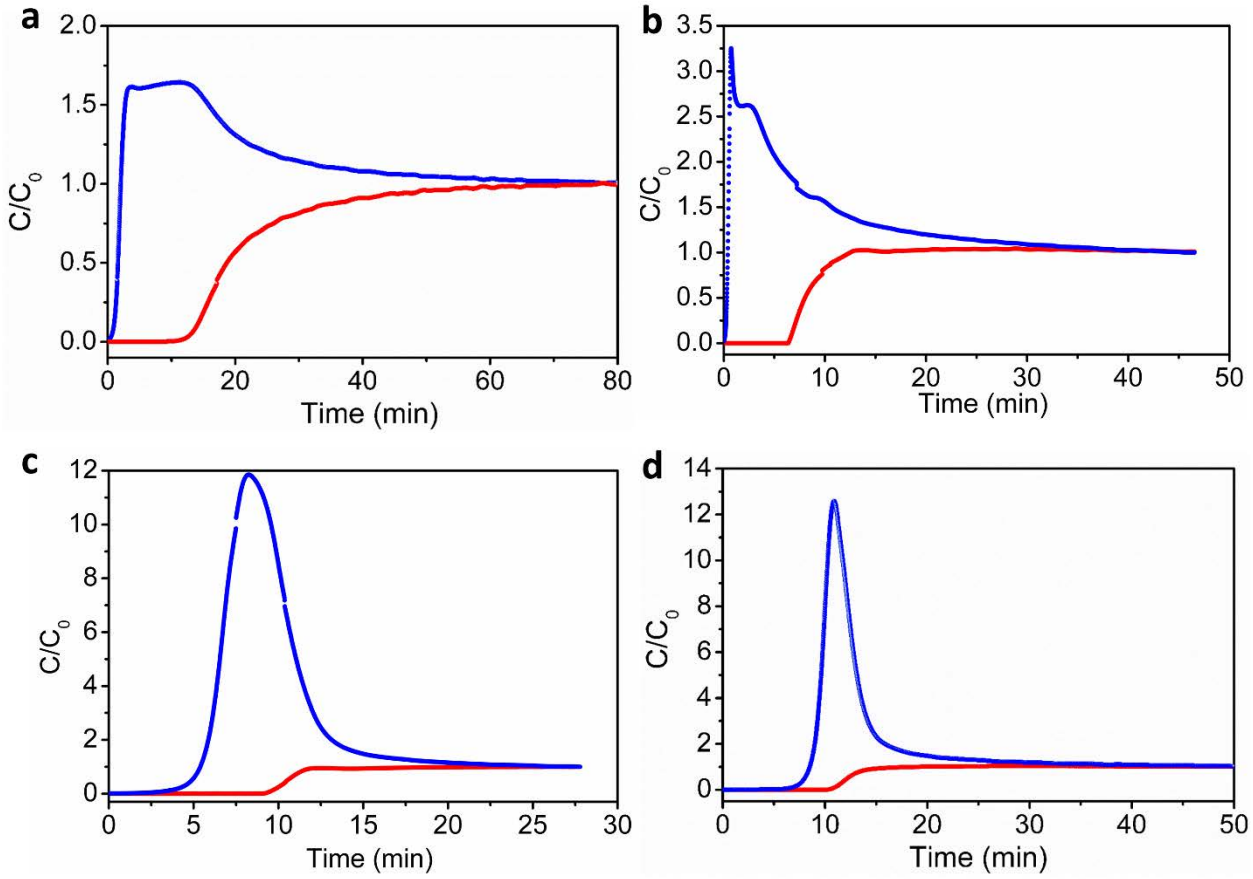

Figure S12. Breakthrough curves for binary mixtures of propane and propylene for a) propane: propylene = 50:50 (total flow rate: 1.6 cc min^{-1}), b) propane: propylene = 50:50 (total flow rate: 4 cc min^{-1}), c) propane: propylene = 10:90 (total flow rate: 1.6 cc min^{-1}), d) propane: propylene = 5:95 (total flow rate: 1.6 cc min^{-1})

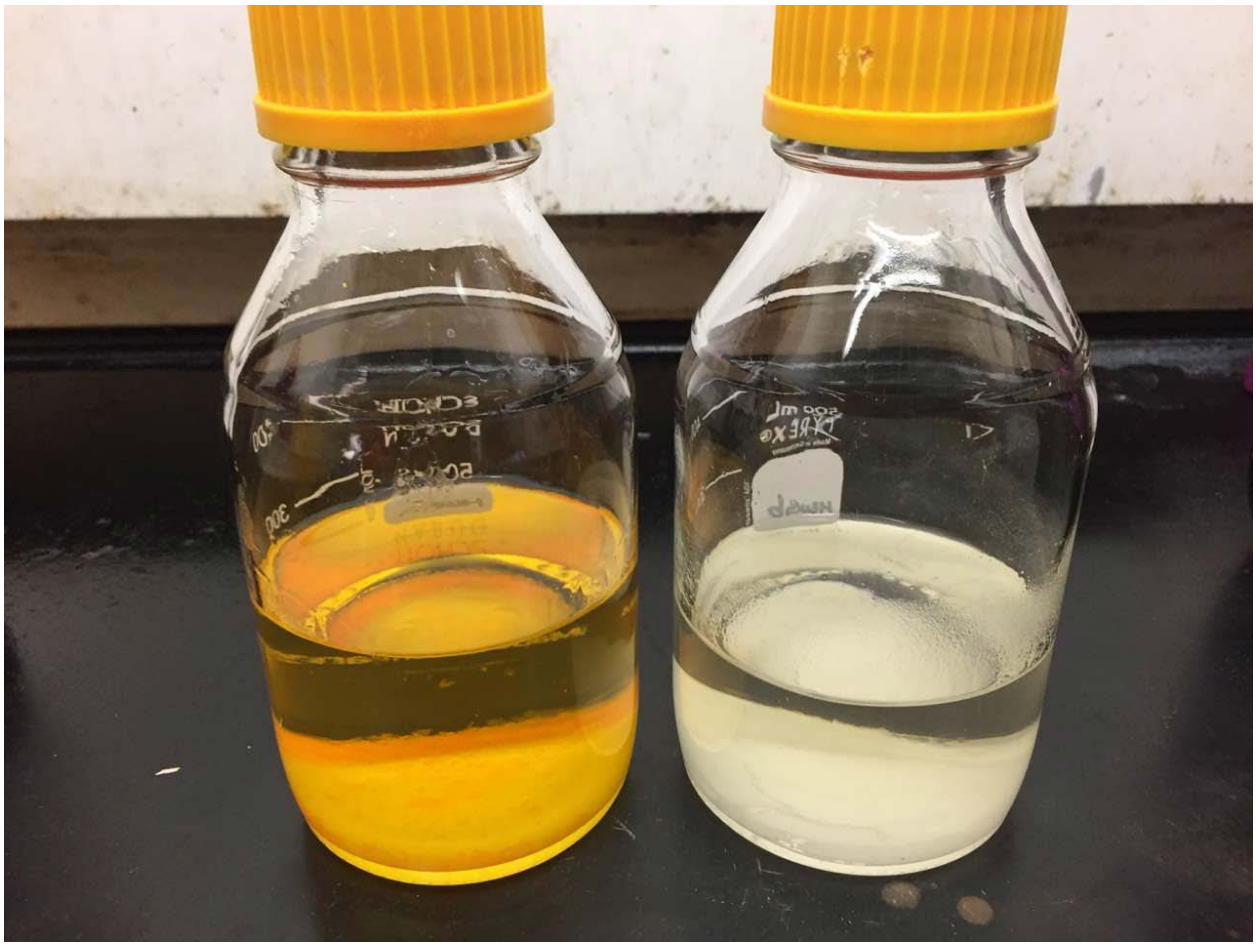

Figure S13. Gram scale synthesis of Y-abtc (left) and Y-bptc (right).

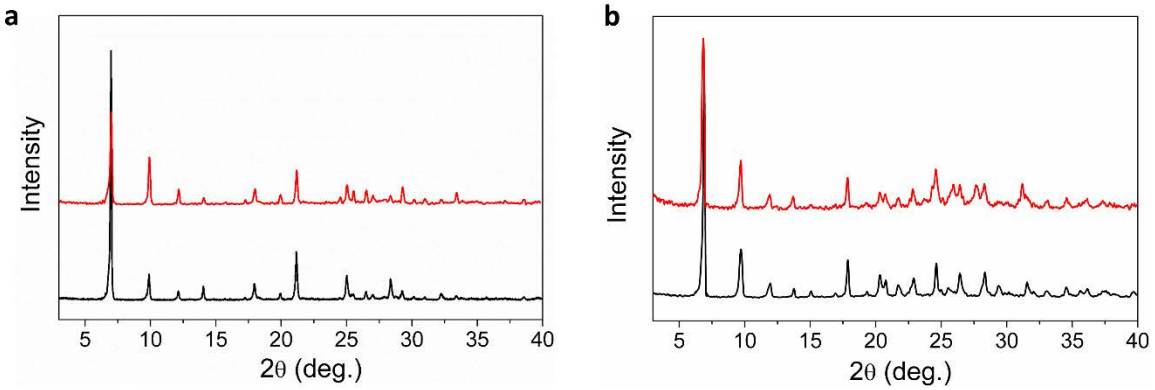

Figure S14. PXRD patterns of a) Y-bptc and b) Y-abtc synthesized with small scale (black, starting with 38.3 mg $Y(NO_3)_3 \cdot 6H_2O$) and 50× scaled up (red).

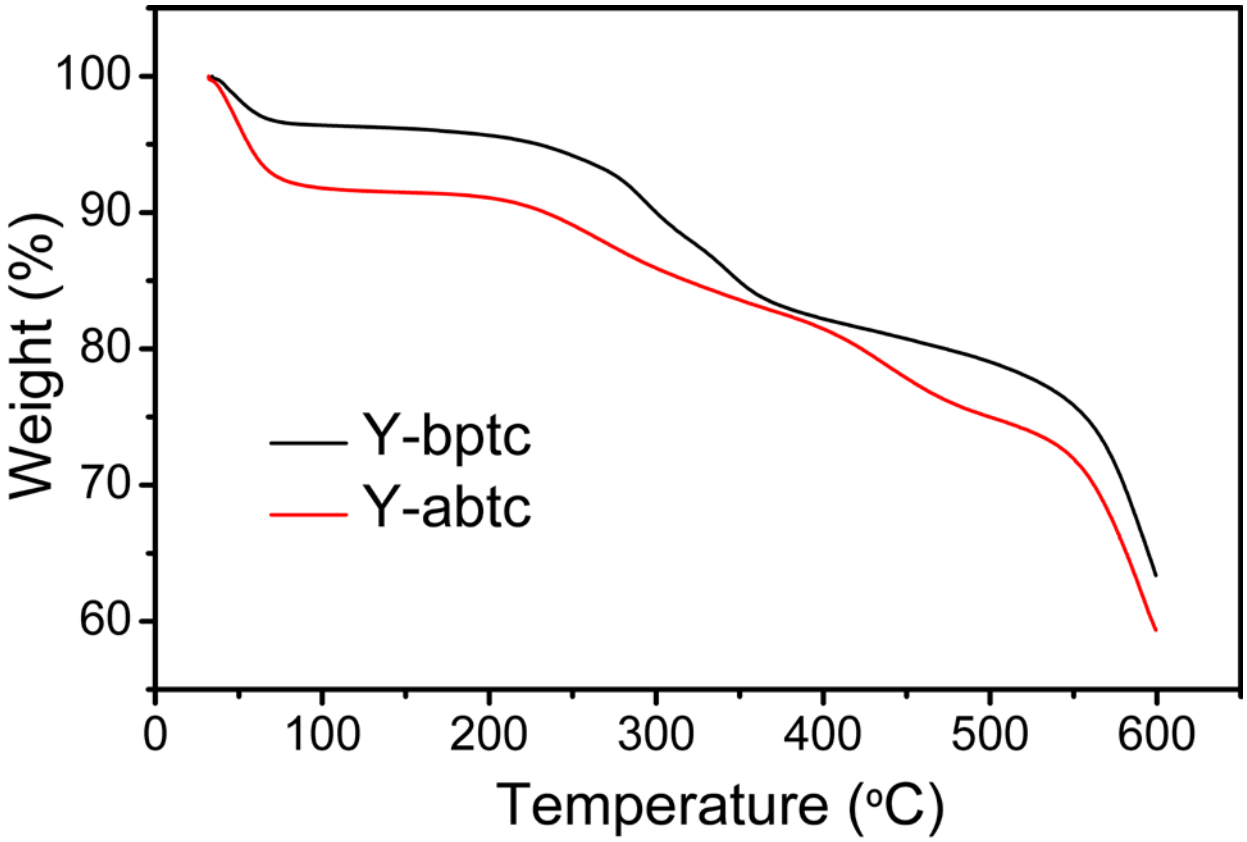

Figure S15. TGA curves for Y-bptc and Y-abtc.

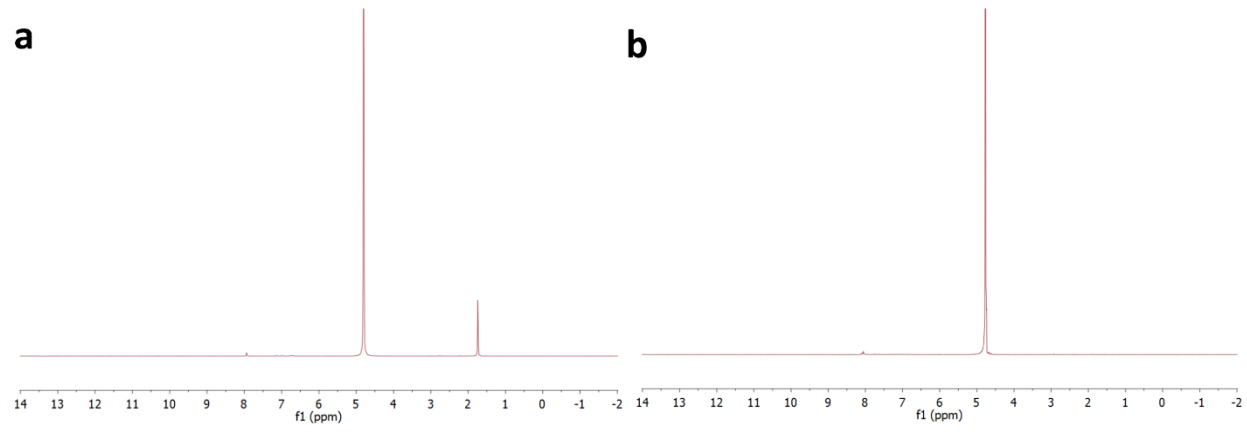

Figure S16. NMR spectra of base digested Y-abtc activated at a) 200 °C and b) 300 °C. The activated MOF was digested in NaOD (1 mmol/L in D_2O).

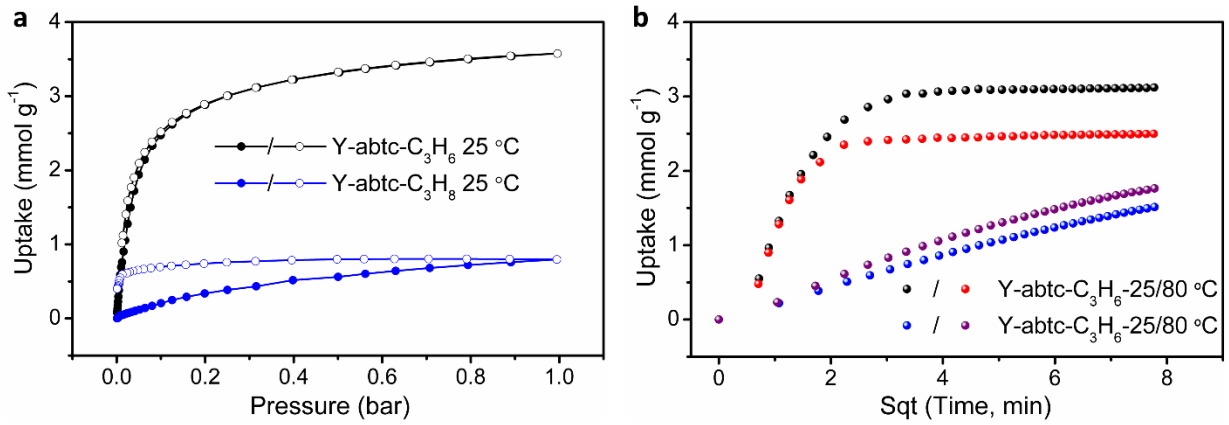

Figure S17. a) Adsorption isotherms and b) adsorption rates at 25 and 80 °C for Y-abtc activated at 300 °C.

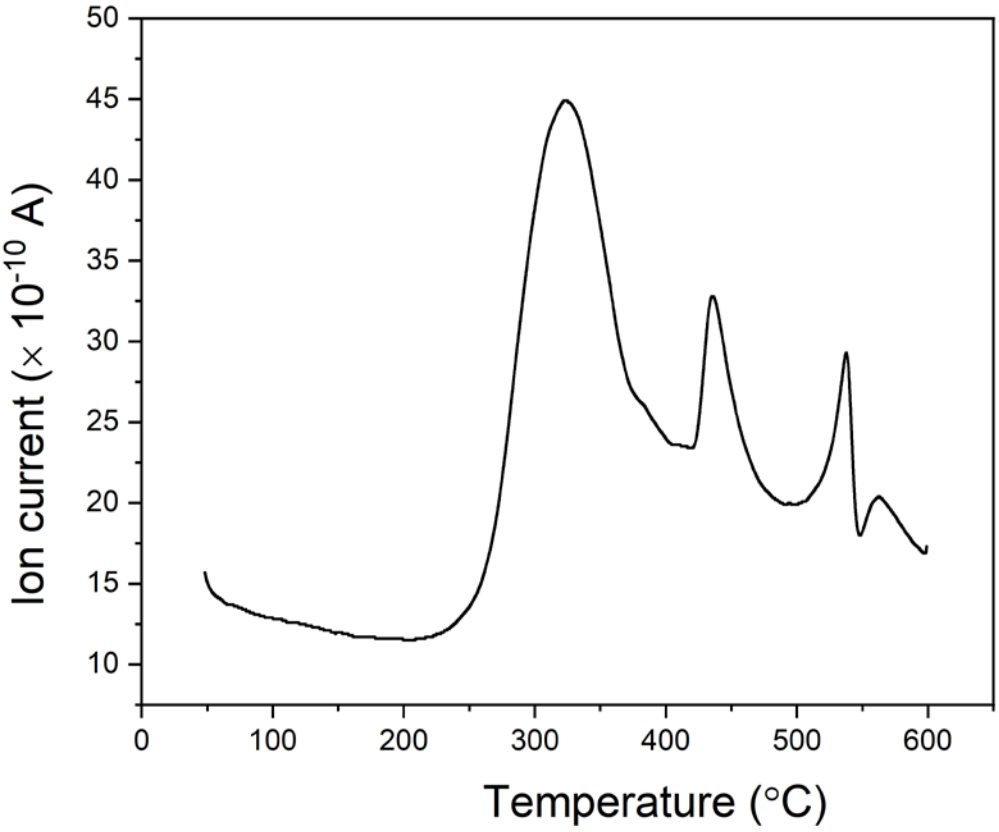

Figure S18. TG-MS spectrum for m= 45.